JOURNAL OF MATERIALS SCIENCE 28 (1993) 2007–2012

The fracture stress of float glass

K. M. ENTWISTLE
Manchester Materials Science Centre, University of Manchester/UMIST, Grosvenor Street, Manchester MI 7HS, UK

A fracture test [1] which uses concentrically loaded square plates supported near their corners has been used to measure the fracture stress of float glass. The plates were 102 mm square and 5.98 mm thick. The maximum displacement at fracture was less than 0.4 mm. Under these circumstances it has been shown that use of a linear finite element solution for the stress distribution and the plate deflections is justified. The glass plates had greater edge damage than had the alumina plates tested in an earlier investigation. In order to secure an adequate proportion of failures in the central plate region, it was necessary to move the supports inwards towards the centre of the plate. This reduced the ratio of the maximum edge stress to the maximum stress in the plate. Batches of plates were tested with loading circle diameters of 7.5 and 25 mm, to measure volume effects, with the side of the plate that had been in contact with the liquid tin in tension. Median ranking was used in the statistical analysis and edge failures were treated as suspensions, it being assumed that the minimum fracture stress of the central region of the edge-fractured plates was the plate centre stress at the fracture load. The Weibull modulus was determined by a linear regression in which extreme members of the population were given reduced weighting using the relationship of Faucher and Tyson [3]. The average fracture stresses were 147.2 and 107.3 N mm^{-2} for the 7.5 and 25 mm loading circles, respectively, and the Weibull moduli were 4.49 and 5.44. These data are shown to agree well with Weibull statistics. Tests using a 7.5 mm diameter loading circle on plates with the non-tin side in tension gave a significantly higher average fracture stress of 242.1 N mm^{-2}, confirming the fact that the non-tin side has a higher strength.

1. Introduction

A previous paper [1] described the development and application of a fracture test based on concentrically loaded square plates supported near the corners. The test was used to measure the effect of stressed volume on the average fracture stress of alumina. The results were shown to be consistent with the predictions of the Weibull analysis. The plates used in that investigation were 1 mm thick and 103 mm square and the deflections at the point of fracture were about 3 mm. Thus the conditions were geometrically non-linear, and for this reason a non-linear ABAQUS finite element analysis was used to determine the stress distribution.

The work described here was carried out on float glass plates. The objectives were two-fold: to explore the validity of the test for fracture stress measurements on glass and to use specimens of a lower aspect ratio than those used in the previous investigation on alumina to gauge if linear theory would yield adequately accurate stress and deflection data for these conditions. The loading arrangement is shown in Fig. 1.

The glass plates were 102 mm square and 5.98 mm thick. They were cut from float glass sheet and the side of the plate that had been in contact with the liquid tin was identified. The deflections at fracture were never greater than 0.4 mm, which is about one-fifteenth of the plate thickness, so conditions would be expected to approach linearity.

A significant feature of the glass plates is that the edge damage is much more severe than was the case with the alumina plates. In consequence, with the supports at the plate corners, about one-third of a small batch of plates fractured with the origin at the middle of the plate edge for a loading circle diameter of 25 mm. Fortunately, it is possible to reduce the ratio of the edge stress to the maximum stress in the plate (which occurs on the loading circle) by moving the corner supports towards the centre of the plate along the plate diagonals. This was done, and it achieved test results in which over 90% of the plates fractured in the highly stressed central region.

2. Plate stresses and deflections

The main series of tests were carried out on glass plates 102 mm square and 5.98 mm thick supported at four points each 42.5 mm from the centre of the plate along a plate diagonal.

The stress distribution and the deflection of this configuration with loading circle diameters of 7.5 and

0022–2461

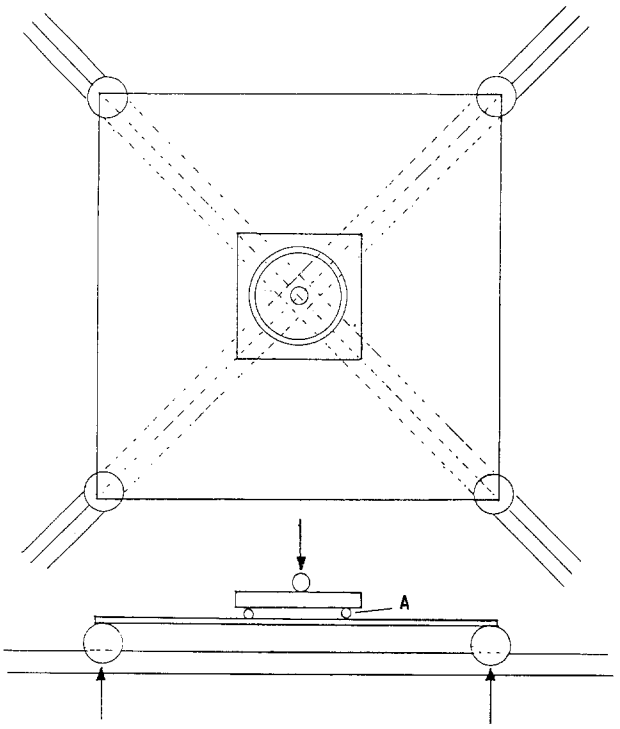

Figure 1 Diagram showing the concentric loading system for the plate. A is a neoprene "O" ring. The supports are shown at the corners. They are moved radially inwards if it is necessary to reduce stress at the plate edges.

25 mm were determined using the ABAQUS finite element package. Both linear and non-linear solutions were obtained. In the investigation reported earlier [1], the finite element solutions for the stresses and deflections were compared with experimental values. The agreement was excellent. Similar comparisons to be reported separately on aluminium plates, of geometry similar to that of the glass plates that are our present concern, showed similar agreement. On the strength of this evidence it was decided to use the finite element solutions to analyse the fracture tests described here. The finite element meshes used in the calculations for the 7.5 and 25 mm diameter loading circles were identical to those reported earlier [1].

Table I gives a measure of the degree of geometrical non-linearity at loads in the range of the fracture loads of the plates. It compares the linear and non-linear solutions for the tensile stress at the centre of the plate, the maximum tensile stress in the plate, which is on the loading circle, the stress in the middle of the edge of the plate and the central deflection. In addition, as a sensitive indicator of non-linearity, it compares the lower surface tensile stress and the upper surface compressive stress at the three positions on the plate. In the linear case these are equal, indicating an absence of membrane stress.

The departure from linearity is seen to be quite small. The predicted central deflections differ by at most about 0.1% and the maximum tensile stress, which is particularly relevant to fracture analysis, is predicted by linear theory with an error less than 1%. We shall later compare the result of analysing the fracture data using the linear and the non-linear solutions.

Individual plates were fractured and the fracture load was recorded. The polar coordinates (r, θ) of the fracture origin were measured. The origin of r was the centre of the plate; the origin of θ was a line from the centre of the plate to the mid-point of the plate edge. The maximum tensile principal stress on the tensile face of the plate at the fracture origin was determined from stress calibration curves of which Figs 2 and 3 are typical. They give the distribution of maximum tensile principal stress as a function of r, the distance from the centre of the plate, for $\theta = 0°$, 15°, 30° and 45°. This region replicates eight times to form the total plate. Fig. 2 is for a loading circle of 7.5 mm diameter and Fig. 3 is for a diameter of 25 mm. The loads correspond to the upper range of the observed fracture loads. Sets of similar curves for a range of applied loads were calculated, but it was found that adequate accuracy in the determination of fracture stress could be obtained by using a calibration curve for a load close to the average fracture load of the batch of plates tested and multiplying the stress by the ratio of fracture load to calibration load. It is seen that the stress is almost independent of θ within the loading circle. Outside the circle the stress is more dependent on θ for the 25 mm diameter loading circle than for the 7.5 mm circle.

The stress solutions were used to evaluate the Weibull stress integrals in order to arrive at the effective areas of the plate. It was concluded from the previous investigation that area integrals gave almost

TABLE I 102 nm square plates, thickness 5.98 mm, elastic modulus, 70,000 N mm^{-2}, Poisson's ratio 0.22, supports 42.5 mm from centre of plate

Loading circle diameter (mm)	Load (N)	Solution	Centre Stress (N mm^{-2})	Max. stress (N mm^{-2})	Max. edge stress (N mm^{-2})	Central deflection (mm)
7.5	4000	Linear	170.1	170.6	55.45	0.2878
		Non-linear				
		Tensile face	171.2	171.6	54.03	0.2875
		Compressive face	− 168.8	− 169.3	− 56.81	
25	6000	Linear	135.9	140.3	79.29	0.3603
		Non-linear				
		Tensile face	137.4	141.3	76.71	0.3597
		Compressive face	− 134.0	− 138.9	− 81.73	

TABLE II Values of K_{A2} (see Equation 2) and effective diameter, d_e, of concentrically loaded plates 102 mm square, thickness 5.98 mm, with corner supports 42.5 mm from the plate centre; $E = 70000\ \text{N mm}^{-2}$, $\nu = 0.22$

Loading article diameter (mm)	m	Load (N)	K_{A2}		d_e (mm)
			Non-linear solution	Linear solution	
7.5	4.5	4000	0.043 38	0.043 61	16.9
	5		0.037 53	0.037 68	15.8
	5.5		0.033 19	0.033 28	14.8
	6		0.029 88	0.029 93	14.1
	6.5		0.027 31	0.027 33	13.4
	7		0.025 26	0.025 26	12.9
	7.5		0.023 60	0.023 59	12.5
	10		0.018 58	0.018 55	11.1
	15		0.014 69	0.014 63	9.9
25	4.5	6000	0.203 2	0.205 3	36.7
	5		0.187 6	0.189 3	35.2
	5.5		0.174 8	0.176 1	34.0
	6		0.164 2	0.165 0	33.0
	6.5		0.155 2	0.155 7	32.1
	7		0.147 6	0.147 7	31.3
	7.5		0.140 9	0.140 8	30.5
	10		0.117 6	0.116 5	27.9
	15		0.092 8	0.090 7	24.8

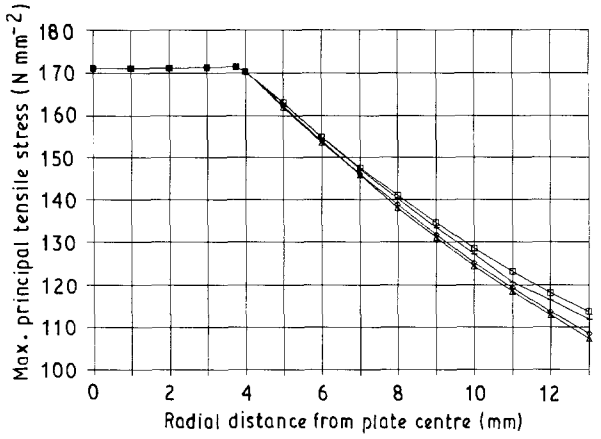

Figure 2 Radial variation of maximum principal tensile stress in glass plates 102 mm square ×5.98 thick. $E = 70000\ \text{N mm}^{-2}$, $\nu = 0.22$, load 4000 N. (□) $\theta = 0°$, (+) $\theta = 15°$, (◇) $\theta = 30°$, (△) $\theta = 45°$. Loading circle diameter 7.5 mm. Supports 42.5 mm from centre of plate on plate diagonals.

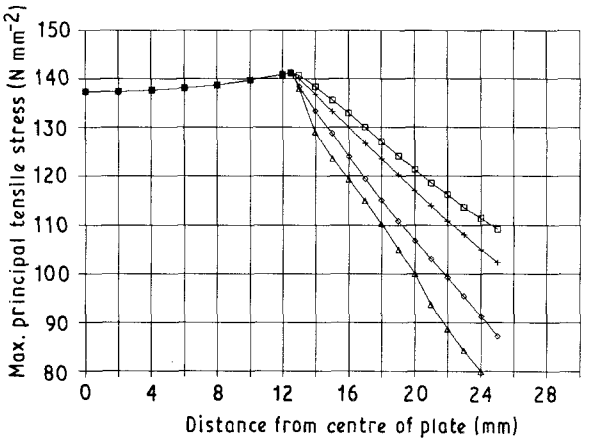

Figure 3 Radial variation of maximum principal tensile stress in glass plates 102 mm square ×5.98 thick. $E = 70000\ \text{N mm}^{-2}$, $\nu = 0.22$, load 6000 N. (□) $\theta = 0°$, (+) $\theta = 15°$, (◇) $\theta = 30°$, (△) $\theta = 45°$. Loading circle diameter 25 mm. Supports 42.5 mm from centre of plate on plate diagonals.

as good a prediction of volume effects as volume integrals, so the area integrals were used also in this work.

The effective area of the tensile face of the plate is

$$A_{E2} = K_{A2} A_0 \tag{1}$$

where A_0 is the total area of the tensile face and

$$K_{A2} = \sum_{i=1}^{N} \left(\frac{\sigma_{i1}^m + \sigma_{i2}^m}{\sigma_p^m} \right) \frac{\Delta A_i}{A_0} \tag{2}$$

σ_{i1} and σ_{i2} are the tensile principal stresses at the ith node in the mesh and σ_p is the maximum tensile stress in the plate, m is the Weibull modulus. ΔA_i is the effective area of the plate associated with the ith node and is obtained by summing the appropriate proportion of the areas of all the elements that meet at the node in question. It is implicit in Equation 1 that σ_{i1} and σ_{i2} contribute independently to the fracture probability. To minimize the volume of computation the value of K_{A2} was determined for one-eighth of the plate, which is replicated, alternately in mirror image, to form the whole plate.

Table II lists the computed values of K_{A2} for a range of values of m, for loading circle diameters of 7.5 and 25 mm and it compares the values derived from the linear solution with those from the non-linear solution at loads in the range of the fracture loads of the plates. The linear solution is a very good approximation to the true value of K_{A2} at the fracture loads.

Included in Table II is an effective diameter, d_e, which is the diameter of a circular plate stressed in equal biaxial tension, at a level equal to the maximum stress in the square plate, which would have the same

fracture probability as the square plate. It should be compared with the appropriate loading circle diameter, because it is an index of the extent to which the region of the square plate outside the loading circle contributes to the fracture probability. It is evident that d_e converges on the loading circle diameter as m increases.

3. Fracture tests

Two batches of plates were tested with loading circle diameters of 7.5 and 25 mm, both with the surface of the plate that had been in contact with the liquid tin in tension. This is the weaker face of the plate. The top compressive face of the plate was covered with adhesive plastic film 50 μm thick to retain the fracture pieces and to facilitate the location of the fracture origin. Typical fracture patterns are shown in Fig. 4. Small pads of plastic film were stuck on the tensile face of the plate at the points of contact of the corner supports in order to reduce Hertzian stresses. The plates were extremely flat so it was not necessary to use shims to bring the four supports into contact with the plate at zero load.

The batch of plates fractured with a loading circle diameter of 7.5 mm comprised 49 specimens. Five of these fractured at major flaws well outside the loading circle. These were rejected. One plate fractured with an initiation site at the edge. Because this is a small proportion of the 43 plates that fractured normally in the central region, it was also ignored.

The batch fractured with a 25 mm diameter loading circle comprised 51 plates. Three fractured at major flaws and were ignored. Eight fractures initiated at the plate edge. 40 plates fractured normally in the central region. It should be noted that the ratio of edge stress to the maximum stress is higher for the 25 mm loading circle than for the 7.5 mm circle. So a higher incidence of edge failures is probable in the 25 mm tests. Although the eight edge fractures are a small proportion of the batch of 48 it would be unwise statistically to ignore them. They were treated as suspensions [2]. We now discuss an appropriate treatment.

It was evident that the fracture loads for the plates in which fracture started at the plate edge with a 25 mm diameter loading circle were in the upper half of the ranked order of fracture loads for the 48 plates. This suggests that the reason for the edge fractures is that the central region of the plates had a higher than average fracture stress, but the edge strength, depending as it does on flaws introduced by cutting, is not related to the strength of the central plate region. So strong plates are more likely to fail at the edge. This tendency removes some samples selectively from the higher fracture stress range of the distribution. The formal way of treating the edge fractures as suspensions would be to place them in the ranking order at stresses equal to the edge stress at the fracture load. This would put all the eight plates below the lowest rank of the 40 plates that fractured normally, which is not realistic. If reduced edge damage had permitted them to fracture normally, the fracture origin would have been quite close to the region of maximum stress in the plate. Accordingly, the following procedure was adopted.

The "normal" plates were ranked according to their fracture stress and the edge fractures were interleaved into this order at stresses corresponding to the stress at the centre of the plate at the load at which the edge fracture occurred. This is considered to be a realistic estimate of the lower limit of the strength of the body of the edge-fractured plates.

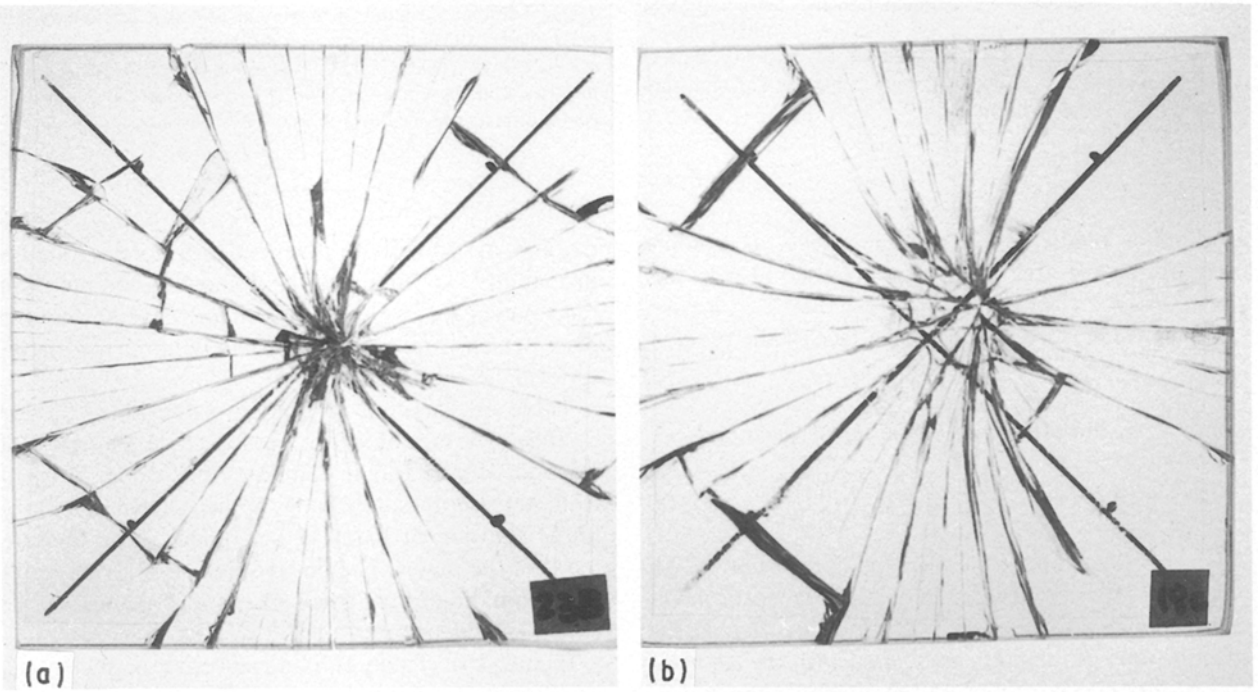

Figure 4 Typical fracture patterns for 102 mm square × 5.98 mm thick glass plate. (a) Loading circle diameter 7.5 mm, (b) loading circle diameter 25 mm. In both cases the fracture origin is close to the loading circle.

Where no suspensions existed, the specimens were ranked in order of increasing fracture stress. Median ranking was used. The median rank was derived from the rank order i from

$$\text{median rank } \phi = \frac{i - 0.3}{n - 0.4} \quad (3)$$

where n is the number of specimens. ϕ is identical to the cumulative fracture probability, P_f.

Where suspensions were included, the increment of rank order number when a suspension occurred was computed from [2]

$$\text{increment} = \frac{(N + 1) - \text{previous sample order number}}{1 + \text{remaining sample size}} \quad (4)$$

where N is the total number of samples, including the suspensions. The remaining sample size includes both suspensions and the failure being considered. The rank order i for a particular failed specimen was obtained by summing all the preceding increments. The median rank was then determined from i using

$$\text{median rank } \phi = \frac{i - 0.3}{N - 0.4} \quad (5)$$

Weibull statistics predict that the survival probability, P_s, of a batch of identically sized specimens similarly stressed is given by

$$\frac{1}{P_s} = \exp\left(\frac{\sigma}{\sigma_0}\right)^m \quad (6)$$

where σ is the fracture stress and σ_0 depends on the volume of the specimen and the stress distribution

$$\ln\ln\left(\frac{1}{P_s}\right) = m\log\sigma - m\log\sigma_0 \quad (7)$$

so a plot of $\ln\ln(1/P_s)$ against $\ln\sigma$ will give m, and $1/P_s = 1/(1 - \phi)$, where ϕ is both the median rank and the cumulative fracture probability.

To obtain m, a linear regression analysis was performed in which the data points were weighted in the manner proposed by Faucher and Tyson [3]. This gives reduced weights to the extreme members of the population.

The weighting factor for the ith specimen was

$$w_i = 3.3\phi_i - 27.5[1 - (1 - \phi_i)^{0.025}] \quad (8)$$

If the regression line is $y = a + bx$, where $y \equiv \ln\ln(1/P_s)_i$ and $x \equiv \ln\sigma_i$, a and b were derived from

$$a = \frac{\sum_n w_i x_i^2 \sum_n w_i y_i - \sum_n w_i x_i \sum_n w_i x_i y_i}{\sum_n w_i \sum_n w_i x_i^2 - \left[\sum_n w_i x_i\right]^2} \quad (9)$$

and

$$b = \frac{\sum_n w_i \sum_n w_i x_i y_i - \sum_n w_i x_i \sum_n w_i y_i}{\sum_n w_i \sum_n w_i x_i^2 - \left(\sum_n w_i x_i\right)^2} \quad (10)$$

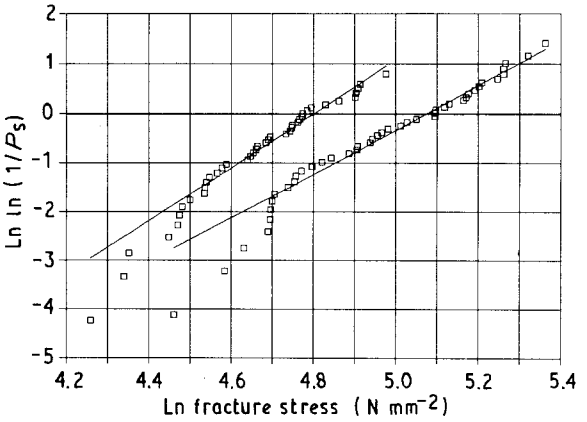

Figure 5 Weibull plots of fracture stress of 102 mm square × 5.98 mm thick glass plates fractured with the tin side of the plate in tension. Supports 42.5 mm from plate centre on plate diagonals. Left-hand set of data are for a loading circle diameter of 25 mm. The set comprises 48 specimens including eight suspensions. The line was calculated by a linear regression. $\bar{\sigma}_f = 107.3\ \text{N mm}^{-2}$, $m = 5.44$. Right-hand set of data are for a loading circle diameter of 7.5 mm. The set comprises 43 specimens with no suspensions. $\bar{\sigma}_f = 147.2\ \text{N mm}^{-2}$, $m = 4.49$. The fracture stresses were determined using the non-linear ABAQUS finite element solution.

TABLE III Glass plates 102 mm square × 5.98 mm thick stressed with the tin side in tension.

Loading diameter (mm)	Average fracture stress (N mm^{-2})	Weibull modulus, m
7.5	147.2	4.49
25	107.3	5.44

4. Fracture data

Weibull plots for plates fractured with the tin side in tension are displayed in Fig. 5 for loading circle diameters of 7.5 and 25 mm. The average fracture stress of the plates fractured with a 7.5 mm loading circle is higher, reflecting the lower stressed volume. The Weibull moduli and the average fracture stresses are listed in Table III.

If the edge fractured plates are ignored and a Weibull analysis is carried out incorporating only the plates that fractured centrally, the Weibull moduli would be 4.49 and 6.28 for 7.5 and 25 mm loading diameters, respectively. These reflect the wider spread in the 25 mm distribution when edge fractures are incorporated as suspensions.

Weibull analysis predicts that the effect of stressed volume, or stressed area in this case, on the average fracture stress is given by

$$\bar{\sigma}_f^m A_E = \text{constant} \quad (11)$$

where A_E is the effective area of the specimen. Now $A_E = K_{A2} A_0$ and K_{A2} is defined in Equation 2, so if A_0 is constant

$$\bar{\sigma}_f^m K_{A2} = \text{constant} \quad (12)$$

so if $\bar{\sigma}_{f25}$ is the average fracture stress for specimens fractured with a 25 mm diameter loading circle and

$\bar{\sigma}_{f7.5}$ is the corresponding value for the 7.5 mm loading circle

$$\bar{\sigma}_{f7.5} = \bar{\sigma}_{f25}\left(\frac{K_{A2\,25}}{K_{A2\,7.5}}\right)^{1/m} \quad (13)$$

The values of K_{A2} are drawn from Table II, whence, using the average of the two m values, 4.97,

$$\bar{\sigma}_{f7.5} = 107.3\left(\frac{0{\cdot}1876}{0.03753}\right)^{1/4.97}$$

$$= 148.32\ \mathrm{N\,mm^{-2}} \quad (14)$$

This is very close to the observed value of 147.2 $\mathrm{N\,m^{-2}}$, so Weibull statistics accurately predict the observed volume dependence.

It is interesting to note that the linear finite element analysis predicts Weibull constants that are very close to those yielded by non-linear theory. Table IV lists the values corresponding to those in Table III derived from the linear stress analysis. So for plates of the aspect ratio and fracture stress level used in the work described here a linear finite element solution for the stresses is acceptable.

Finally, a batch of plates was tested with the face that was not in contact with the liquid tin in tension. It is known that the tin side and the non-tin side are not of equal strength. A small batch of specimens was fractured with a loading circle diameter of 7.5 mm and supports 42.5 mm for the centre of the plate. A third of the batch fractured at the edge, because of the high strength of the central plate region. As the supports are moved inwards the ratio of maximum edge tensile stress to maximum tensile stress in the plate falls, as Table V shows. A significant reduction of edge failures was produced by moving the corner supports to a position 35 mm from the plate centre. In a batch of 33 specimens, fractured with a loading circle diameter of 7.5 mm, five samples failed by fracture initiated at the edge. This is a satisfactory improvement.

The stress at the point of fracture origin in the 28 samples that failed in the central region was determined from a non-linear finite element solution. The edge fractures were treated as suspensions and were placed in the fracture stress ranking order at a stress equal to the stress at the centre of the plate at the edge fracture load. Fig. 6 is a Weibull plot of the data. The average fracture stress for the batch is 242.1 $\mathrm{N\,mm^{-2}}$ and the Weibull modulus 5.53, which is close to the range of the two values for the tests with the tin side in tension. The average facture stress of 242.1 $\mathrm{N\,mm^{-2}}$ is significantly higher than the corresponding value for the tin side, 147.2 $\mathrm{N\,mm^{-2}}$, confirming the difference of strength of the two faces.

TABLE IV

Loading diameter (mm)	Average fracture stress ($\mathrm{N\,mm^{-2}}$)	Weibull modulus, m
7.5	146.3	4.48
25	106.2	5.43

TABLE V Ratio of maximum edge stress to maximum tensile stress in 102 mm square plates 5.98 mm thick at loads comparable with the fracture loads (3000–7000 N)

Loading circle diameter (mm)	Distance of supports from plate centre		
	50 mm	42.5 mm	35 mm
7.5	0.400	0.315	0.225
25	0.656	0.550	0.417

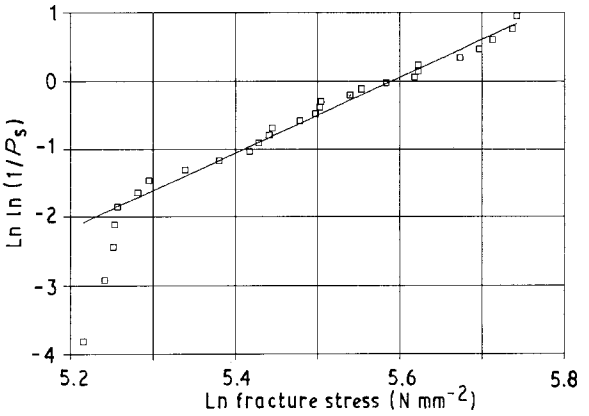

Figure 6 Weibull plot of the fracture stress of 102 mm × 5.98 mm thick glass plates fractured with the non-tin side in tension. Loading circle diameter 7.5 mm and supports 35 mm from plate centre on the plate diagonals. The set comprises 33 plates including five suspensions. Uses non-linear ABAQUS finite element solution. $\bar{\sigma}_f = 242.1\ \mathrm{N\,mm^{-2}}$, $m = 5.53$.

Acknowledgements

The author thanks Dr A. Ledwith, Director of Research of Pilkington plc, for the supply of glass plates, Mr. H. W. Mackenzie, Dr. P. Ramsey for stimulating discussions, and Mr D. Oakley, who shared his own research findings and was helpful with statistical data analysis.

References

1. K. M. ENTWISTLE, *J. Mater. Sci.* **26** (1991) 1078.
2. C. LIPSON and N. J. SHETH, "Statistical Design and Analysis of Engineering Experiments" (McGraw-Hill, New York, 1973) p. 19.
3. B. FAUCHER and W. R. TYSON, *J. Mater. Sci. Lett.* **7** (1988) 1199.

Received 9 August
and accepted 8 October 1992